PCCP

Accepted Manuscript

ROYAL SOCIETY OF CHEMISTRY

www.rsc.org/pccp

Journal Name

RSCPublishing

ARTICLE

Combined Activation Strain Model and Energy Decomposition Analysis Methods: A New Way to Understand Pericyclic Reactions

Israel Fernández[a]

Cite this: DOI: 10.1039/x0xx00000x

Received 00th January 2012,
Accepted 00th January 2012

DOI: 10.1039/x0xx00000x

www.rsc.org/

The recently introduced Activation Strain Model (ASM) has allowed us to gain more insight into the intimacies of different fundamental processes in Chemistry. In combination with the Energy Decomposition Analysis (EDA) method, we have nowadays a very useful tool to quantitatively understand the physical factors that govern the activation barriers of reactions within organic and organometallic chemistry. In this Perspective article, we present selected illustrative examples on the application of this method to pericyclic reactions (Diels-Alder and double group transfer reactions) to show that this methodology nicely complements other more traditional, widely used theoretical methods.

Introduction

Pericyclic reactions are highly useful transformations in organic and organometallic synthesis.[1,2] This is mainly due to their well-known ability to increase the molecular complexity in one single reaction-step, very often with high to complete stereoselectivity. For this reason, they are usually involved in the preparation of target molecules including complex natural products.

One important feature of pericyclic reactions is that they proceed concertedly through a fully conjugated cyclic transition state. Theory has played an important role to understand the intimacies of these concerted transformations.[3] For instance, Fukui's frontier molecular orbital (FMO) theory[4] and Woodward-Hoffmann rules[5] have become a powerful conceptual framework to interpret the reactivity and regioselectivity patterns in different pericyclic processes such as cycloaddition reactions. In the FMO theory,[6] the interactions of the HOMO and LUMO of reactants are emphasized and the strongest interactions are suggested to occur between orbitals that are closest in energy and which have the largest overlap.[3,6] Despite the usefulness and popularity of the FMO theory, a significant number of deficiencies have been identified, mainly due to the lack of quantitative significance of these FMO interactions.[7] This is mainly ascribed to the fact the FMO interactions are computed at the equilibrium geometries of the involved reactants therefore ignoring those interactions occurring at the transition state region or at any other point along the reaction coordinate.

Fortunately, the advent of Density Functional Theory (DFT) and the impressive development of Computational Chemistry in the last decades have led to new conceptual models aimed at a deeper understanding of the molecular reactivity. Among them, conceptual density functional (DFT) and Hard and Soft Acid and Base (HSAB) theories,[8] valence bond (VB) analyses[9] or Marcus Theory[10] have also contributed to our current understanding of fundamental processes in chemistry.

In this Perspective article, we shall focus on the combination of the *Activation Strain Model* (ASM) and the *Energy Decomposition Analysis* (EDA) methods, which provides a robust methodology to explore the trends in reactivity within organic and organometallic chemistry. In particular, we will show how the ASM/EDA method has been quite helpful recently to gain quantitative insight into the physical factors that control the activation barriers in pericyclic reactions. To this end, we will summarize recent illustrative examples, mainly derived from our laboratories, focused on two types of pericyclic reactions, namely Diels-Alder cycloaddition reactions and group transfer processes.

The Methodology: Activation Strain Model and Energy Decomposition Analysis Methods

The relatively recent introduction in 1999 of the so-called *activation strain model* (ASM) has allowed us to gain more insight into the physical factors which control how the activation barriers arise in different fundamental processes.[11] This model is the same as the *distortion/interaction model* proposed by Houk and co-workers in 2007.[12] The method is a fragment approach to understanding chemical reactions, in which the height of reaction barriers is described in terms of the original reactants. The ASM is a systematic further development of the fragment approach from equilibrium structures to transition states (TS) as well as *non-stationary* points, e.g., points along a reaction coordinate. Thus, the potential energy surface $\Delta E(\zeta)$ is decomposed, along the reaction coordinate ζ, into the strain energy $\Delta E_{\text{strain}}(\zeta)$ associated with the structural deformation that the reactants undergo plus the interaction $\Delta E_{\text{int}}(\zeta)$ between these increasingly deformed reactants:

$$\Delta E(\zeta) = \Delta E_{\text{strain}}(\zeta) + \Delta E_{\text{int}}(\zeta)$$

The strain $\Delta E_{\text{strain}}(\zeta)$ is determined by the rigidity of the reactants and on the extent to which groups must reorganize in a particular reaction mechanism. Therefore, this geometrical deformation is characteristic for the reaction pathway under consideration. This term can be, of course, further partitioned into the individual contributions stemming from each of the reactants involved in the process. The interaction $\Delta E_{\text{int}}(\zeta)$ between the reactants depends on their electronic structure and on how they are mutually oriented as they approach each other. It is the interplay between $\Delta E_{\text{strain}}(\zeta)$ and $\Delta E_{\text{int}}(\zeta)$ that determines if and at which point along ζ a barrier arises. This decomposition of the energy $\Delta E(\zeta)$ is carried out along the intrinsic reaction coordinate (provided by the IRC method),[13] i.e. from the separate reactants (or from a weakly bonded reactant complex when it exists) to the reaction products via the corresponding transition state.

According to this model, the activation energy of a reaction $\Delta E^{\ddagger} = \Delta E(\zeta^{\text{TS}})$ consists of the activation strain $\Delta E^{\ddagger}_{\text{strain}} = \Delta E_{\text{strain}}(\zeta^{\text{TS}})$ plus the TS interaction $\Delta E^{\ddagger}_{\text{int}} = \Delta E_{\text{int}}(\zeta^{\text{TS}})$, (see Figure 1).

$$\Delta E^{\ddagger} = \Delta E_{\text{strain}}{}^{\ddagger} + \Delta E_{\text{int}}{}^{\ddagger}$$

This model has successfully contributed to the current understanding of S_N2 and E2 reactions, metal-mediated bond activation, and different pericyclic reactions.[11,12]

The interaction energy between the reactants along the reaction coordinate, $\Delta E_{\text{int}}(\zeta)$, can be further decomposed in meaningful energy contributors with the help of the Energy Decomposition Analysis (EDA) method,[14] which was developed by Ziegler and Rauk[15] following a similar procedure suggested by Morokuma.[16] This method has been proven to give important information about the nature of the bonding in main-group compounds,[17] transition-metal complexes,[18] as well as biological and supramolecular aggregates.[19] Thus, with the help of the EDA, the $\Delta E_{\text{int}}(\zeta)$ can be decomposed into the following energy contributors:

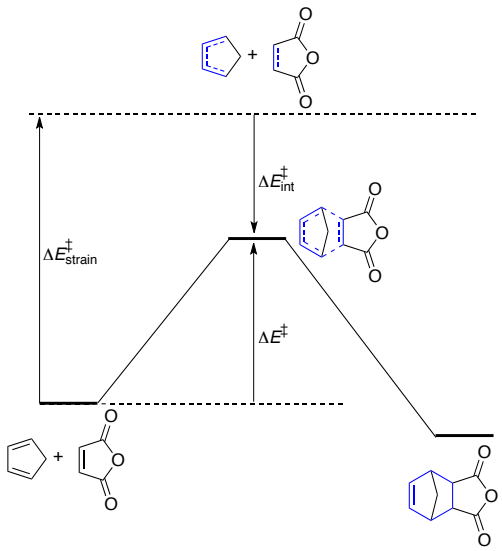

Fig. 1 Illustration of the activation-strain model for the Diels-Alder reaction between cyclopentadiene and maleic anhydride.

$$\Delta E_{\text{int}}(\zeta) = \Delta V_{\text{elstat}} + \Delta E_{\text{Pauli}} + \Delta E_{\text{orb}} + \Delta E_{\text{disp}}$$

The strategy is to divide the system of interest, AB, into fragments, e.g., A and B, which are then recombined in three separate steps in order to obtain the energies of individual interactions. In the first step the fragments, which are calculated with the frozen geometry of the entire system, are superimposed without electronic relaxation yielding the quasiclassical electrostatic attraction ΔV_{elstat}. In the second step the product wave function becomes antisymmetrized and renormalized, which gives the repulsive term ΔE_{Pauli}, termed Pauli repulsion. This term comprises the destabilizing interactions between occupied orbitals and is responsible for any steric repulsion. In the third step the molecular orbitals relax to their final form to yield the stabilizing orbital interaction ΔE_{orb}. This energy contributor accounts for charge transfer (interaction between occupied orbitals on one moiety with unoccupied orbitals on the other, including HOMO–LUMO interactions) and polarization (empty-occupied orbital mixing on one fragment due to the presence of another fragment) and can be further partitioned into contributions by orbitals belonging to different irreducible representations of the point group of the interacting system (when applicable). Finally, ΔE_{disp} takes into account the dispersion forces. The sum of these four terms $\Delta V_{\text{elstat}} + \Delta E_{\text{Pauli}} + \Delta E_{\text{orb}} + \Delta E_{\text{disp}}$ gives the total interaction energy ΔE_{int}. Further details about the EDA method can be found in the literature.[14]

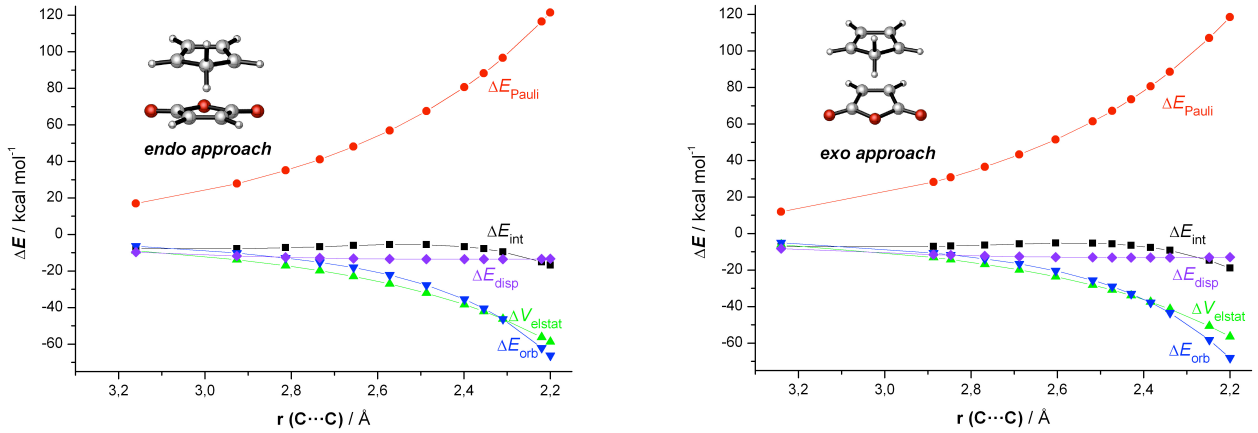

Fig 2. Decomposition of the interaction energy for the Diels-Alder reaction between CP and MA along the reaction coordinate projected onto the C···C bond for the endo (left) and exo (right) pathways. All data have been computed at the BLYP-D3/TZ2P//M05-2X/def2-TZVPP level. See reference 28.

Diels-Alder Reactions

Origin of the "Endo rule"

The Diels-Alder [4+2] cycloaddition reaction is arguably the most representative pericyclic reaction.[20] Interestingly, many Diels-Alder reactions favour the formation of the endo cycloadduct predominantly (or exclusively, in some cases). This preference is known as the "endo rule" according to the empirical formulation by Alder and Stein in 1934.[21]

Although different experimental and theoretical arguments have been presented to account for this endo-preference (i.e. inductive effects,[22] charge transfer[23] or CH···π interactions[24]), there is nowadays general agreement that secondary orbital interactions (SOI),[25] initially proposed by Woodward and Hoffmann,[26] are responsible for the observed stereocontrol. Nevertheless, the magnitude of these SOI is relatively small,[27] therefore suggesting that other factors may be controlling the selectivity of the Diels-Alder cycloaddition reaction. Therefore, we thought that the combination of the ASM method, which has been used for analysing other Diels-Alder processes,[12c,d] in combination with the EDA could provide a definitive rationalization of the empirical endo-rule.[28]

We first focused on the textbook thermal Diels-Alder reaction between maleic anhydride (MA) and cyclopentadiene (CP, see Figure 1), a process which exclusively affords the thermodynamically less stable endo cycloadduct.[29] Our calculations (M05-2X/def2-TZVPP level) clearly confirm that the regioselectivity of the process takes place under kinetic control in view of the lower activation barrier computed for the endo-pathway ($\Delta\Delta G^{\ddagger}_{298}$(endo-exo) = 2.1 kcal/mol). Moreover, the exo-pathway proceeds through a slightly earlier transition state.

Strikingly, and in sharp contrast to the widely accepted orbital interaction-based explanation for the endo rule, the EDA method shows that the interaction energy between MA and CP along the reaction coordinate, $\Delta E_{int}(\zeta)$, appears to be not at all decisive for the endo selectivity (Figure 2). Although ΔE_{int} does favour the endo pathway in early stages of the reaction, at later stages (i.e. at the transition state region), the interaction along the exo pathway is no longer less but even slightly more stabilizing than that along the endo pathway. In this stage, which determines the height of the barrier, the reactants have essentially equally suitable arrangements to enter into favourable bonding interactions at the positions where the two new C–C bonds are being formed. Indeed, the partitioning of the interaction energy given by the EDA clearly indicates that near the TS, the contribution of the orbital term, $\Delta E_{orb}(\zeta)$, which include the SOI, is very similar for both pathways and is even slightly more stabilizing for the exo approach (Figure 2). This leads to the conclusion that it is *not* the orbital interactions, commonly held responsible, that contribute to, let alone cause, the endo selectivity of this Diels-Alder reaction. This finding necessarily implies that other factors constitute the origin of the endo-rule.

In order to gain more insight into the physical factors controlling the barrier heights of the endo and exo cycloaddition reactions, we have applied the ASM to both pathways. From the computed activation strain diagrams depicted in Figure 3, it becomes clear that, at the TS region, the strain energy $\Delta E_{strain}(\zeta)$ (which is associated with deforming the reactants) becomes more destabilizing in the exo-pathway, even though the corresponding transition state is reached earlier. This can be ascribed to the fact that the methylene unit of CP runs into the oxygen atom of the anhydride. Thus, in order to avoid an extreme increase in Pauli repulsion between C–H bonding orbitals and O lone-pair type orbitals, the methylene unit has to bend away significantly from the oxygen, which is translated into a higher (i.e. more destabilizing) strain energy in the exo-pathway. As the interaction energy is similar in both approaches, it can be concluded that the main factor responsible for the endo preference is not the favourable SOI in the endo

transition structure but an unfavourable steric arrangement in the exo pathway.

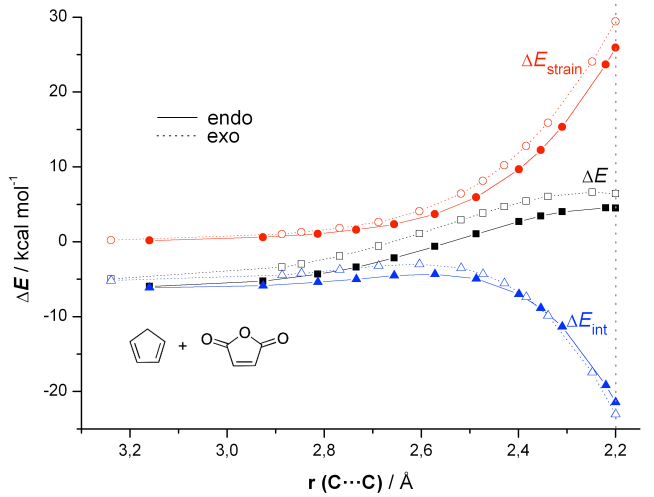

Fig 3. Activation-strain analysis of the endo (solid curves) and exo (dotted curves) Diels–Alder cycloaddition reactions between MA and CP along the reaction coordinate projected onto the forming C···C bond distance. All data have been computed at M05-2X/def2-TZVPP level. See reference 28.

The above findings suggest that the endo selectivity can be reduced by avoiding this unfavourable steric arrangement occurring in the exo-pathway. Indeed, when using *s-cis* butadiene instead of CP as diene in the corresponding DA reaction with maleic anhydride, the computed $\Delta\Delta E_{strain}$(endo-exo) of 3.3 kcal/mol for the reaction involving CP is significantly reduced to 1.7 kcal/mol in the process involving butadiene. As a consequence, the corresponding $\Delta\Delta E^{\ddagger}$(endo-exo) is also reduced, which should be translated into a significant formation of the exo-cycloadduct, as experimentally found (endo/exo cycloadducts ratio of 85:15, at 80 ºC, and 50:50, at 120 ºC).[29]

[6,6]-Selectivity in the Diels-Alder Reaction between C_{60} and cyclopentadiene

The ASM method, in combination with the EDA, has been particularly useful to understand the exclusive formation of the [6,6]- over the [5,6]-cycloadduct in the Diels-Alder reaction between C_{60} and cyclopentadiene.[30]

C_{60}-fullerene possesses two types of bonds: the pyracylenic type [6,6]-bond, where two six-membered rings are fused, and the corannulenic [5,6]-bond, which corresponds to the ring junction between a five- and a six-membered ring.[31] In general, it is well-known that cycloaddition reactions in empty fullerenes show a remarkable (or exclusive) preference towards [6,6]- over [5,6]-bonds.[31,32] However, the reasons behind this well-established experimental (and theoretical) [6,6]-preference were not completely understood. For this reason, we decided to apply the ASM/EDA method to unravel the factors controlling this selectivity.[30]

To this end, the Diels-Alder cycloaddition reaction between C_{60} and cyclopentadiene was selected. In agreement with the available experimental and computational data,[33,34] our calculations reveal that the observed regioselectivity takes place under both kinetic and thermodynamic control, in view of the considerably higher activation energy and less exothermic reaction energy computed for the formation of the [5,6]-cycloadduct (Figure 4). Moreover, the [6,6]-pathway proceeds via an earlier transition state.

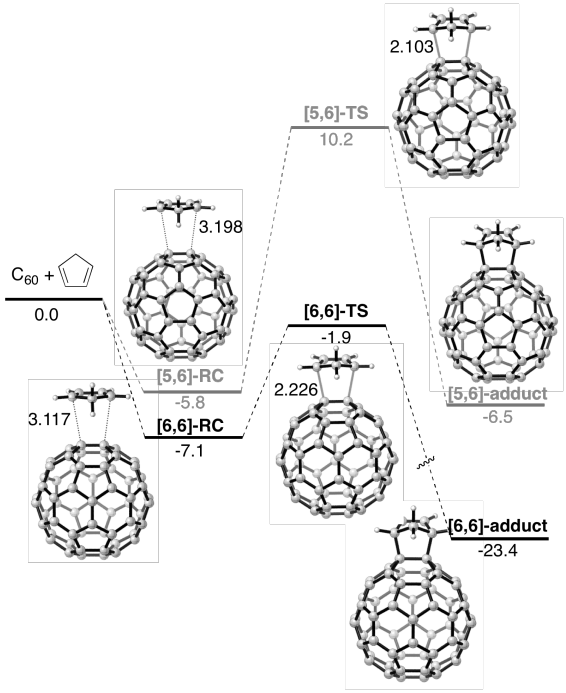

Fig 4. Computed reaction profile of the reaction between cyclopentadiene and C_{60}. Energies are given in kcalmol_1 and bond lengths in angstroms. All data have been computed at the BP86-D3/TZ2P+//RI-BP86-D3/def2-SVP level. See reference 30.

Interestingly, the computed TS interactions, $\Delta E^{\ddagger}_{int}$, between the deformed C_{60} and cyclopentadiene are exactly the same (-21.3 kcal/mol) for the [6,6]- and [5,6]-pathways. These single-point analyses in the TS may, misleadingly, suggest that the reaction profiles of the two pathways differ due to strain whereas the interaction is the same. However, the activation strain diagrams depicted in Figure 5 clearly show that this is not the case.

If we compare both diagrams, we realize that the stronger interaction between the reactants along the entire reaction coordinate in the [6,6]-reaction pathway is the major factor controlling the selectivity of the process. Indeed, the $\Delta E_{int}(\zeta)$ between the deformed reactants is stabilizing from the initial stages of the reaction and becomes more and more stabilizing as one approaches the corresponding transition state. At variance, for the [5,6]-pathway (represented in dotted lines in Figure 5), the reaction profile is initially going up in energy because of a destabilizing interaction $\Delta E_{int}(\zeta)$ between the reactants and inverts at a certain point, after which this term becomes more and more stabilizing as one further approaches the transition state. As a consequence, the [6,6]-transition state is reached earlier than in the [5,6]-pathway and has a lower

strain therefore which, in turn, is translated into a much lower activation barrier.

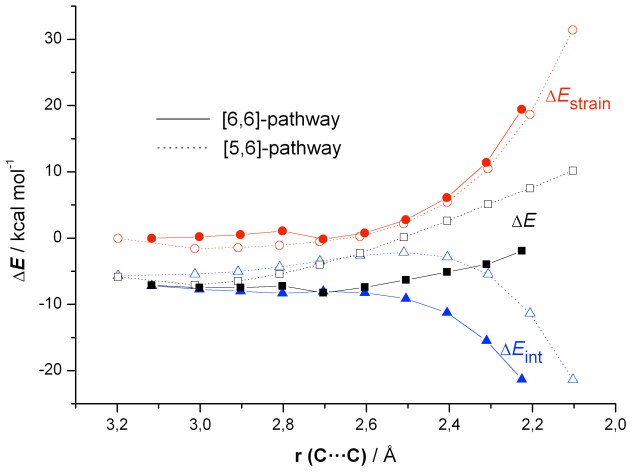

Fig 5. Activation-strain analysis of the [4+2]-cycloaddition reaction between C_{60} and cyclopentadiene along the region comprising the reactant complex and the transition state projected onto the forming C···C bond. Solid lines refer to the [6,6] pathway whereas dotted lines to the [5,6] pathway. All data have been computed at the BP86-D3/TZ2P+//RI-BP86-D3/def2-SVP level. See reference 30.

The partitioning of the interaction energy given by the EDA suggests that, similarly to the observed trend in ΔE_{int}, the orbital interactions measured by ΔE_{orb} are always less stabilizing in the [5,6]-pathway along the reaction coordinate (Figure 6). This is ascribed to the more favourable orientation of the [6,6]-pathway which allows for a much better <HOMO(cyclopentadiene)|LUMO(C_{60})> overlap from the initially formed reactant complex to the corresponding transition state. For instance, the computed overlap reaches its maximum for **[6,6]-TS** (S = 0.106), while a much lower value of S = 0.056 was found for **[5,6]-TS**, despite its shorter C···C bond distance.

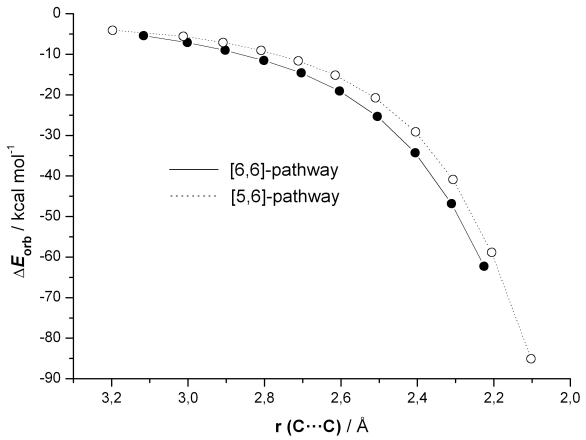

Fig 6. Change in the ΔE_{orb} term for the [6,6]-pathway (solid line) and the [5,6] pathway (dotted line). All data have been computed at the BP86-D3/TZ2P+//RIBP86-D3/def2-SVP level.

Group Transfer Reactions

Double Group Transfer (DGT) Reactions

DGT reactions are a general class of pericyclic reactions which involve the simultaneous migration of two atoms/groups from one compound to another in a concerted reaction pathway.[1] This definition includes textbook reactions like the diimide reduction of double or triple bonds[35] and the Meerwein-Ponndorf-Verley reduction (MPV) of carbonyl groups.[36]

The archetypal DGT reaction is the thermally allowed, concerted and highly synchronous [σ2s+σ2s+π2s] suprafacial transfer of two hydrogen atoms from ethane to ethylene, which occurs through the highly symmetric planar six-membered ring transition structure $\mathbf{TS_{DGT}}$ (Figure 7).[37]

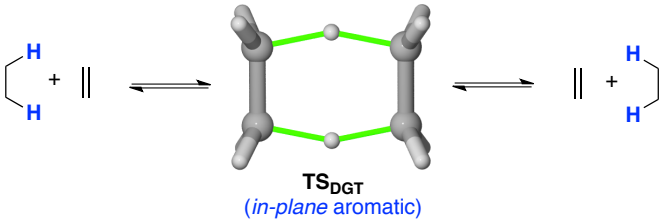

Fig 7. Archetypal DGT reaction between ethane and ethylene.

The occurrence of a planar highly symmetric six-membered transition state, where the C–C bonds have a partial double-bond character and are equalized, is an indication of electronic delocalization within the plane containing the six electrons involved in the process. Indeed, this type of transition states can be considered as *in-plane* aromatic species[38] in view of the computed strongly negative Nucleus Independent Chemical Shifts (NICS)[39] values (in the range of −10 to −25 ppm, depending on the initial substrates) and the presence of a strong diatropic induced current that is delocalized within the molecular plane.[37] Despite the aromatic character of these transition structures, DGT reactions are associated with relatively high barriers (typically $\Delta E^{\ddagger}$ > 40 kcal/mol), which seems contradictory if we consider that a gain in aromaticity is usually translated into a gain in stability.

At this point, the combined ASM/EDA method becomes an extremely helpful tool to understand the origins of the high activation barriers computed for these pericyclic transformations.[40] Figure 8 shows the activation strain diagram for the DGT reaction involving ethane and ethylene. It becomes clear that at the early stages of the process the reaction profile ΔE monotonically becomes more and more destabilized as the reactants approach each other. This initial increase in ΔE is ascribed to the fact that the interaction energy between the deformed reactants (ΔE_{int}) becomes destabilizing at long H···C distances as a consequence of the Pauli repulsion between closed-shells (notably between the C–H bonds of ethane and the π-system of ethene). In addition, the initial increase in ΔE is also caused by the ethane reactant, as it has to adopt the required eclipsed conformation to interact with the π-system of ethene.

This behaviour resembles that found for other pericyclic reactions like Diels-Alder reactions (see above), [3+2]-cycloadditions[41] and Alder-ene processes,[42] but differs from S_N2 or E2 reactions[11] where there exists a potent donor–acceptor interaction between the HOMO of the nucleophile/base and the LUMO of the substrate from the beginning of the process.

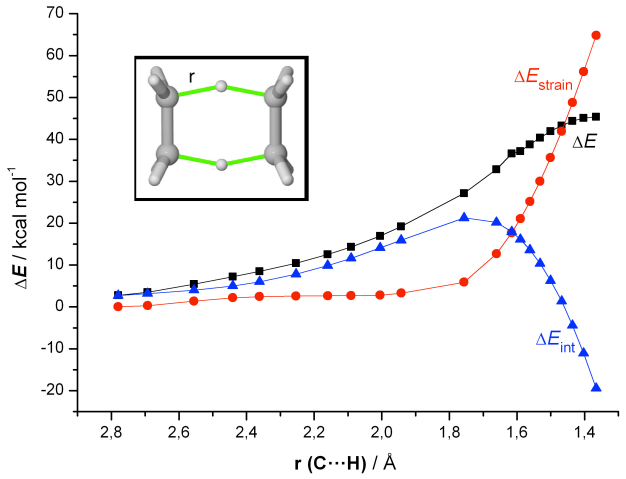

Fig 8. Activation-strain analysis of the DGT reaction between ethane and ethene along the reaction coordinate projected onto the forming C···H bond. All data have been computed at the OLYP/TZ2P level. See reference 40.

If we now further proceed along the DGT reaction coordinate, the trend in ΔE_{int} inverts at a certain point, after which this term becomes more and more stabilizing. This stabilization in the ΔE_{int} curve occurs shortly after the onset of the strain curve. Despite that, the reason that the overall energy ΔE still goes up until the transition state is of course also the increase in the destabilizing strain energy, which clearly compensates the stabilization provided by ΔE_{int}. Therefore, the strain energy the major factor controlling the activation barriers of DGT reactions as ΔE_{strain} becomes highly destabilizing and more than compensates for the gain in aromaticity during the reaction.

Furthermore, the EDA method indicates that the dominant term causing the inversion in ΔE_{int} is the orbital interaction energy ΔE_{orb}, which is not surprising if we take into account the aromatic nature of the transition state (Figure 9). Interestingly, although the electrostatic attraction ΔV_{elstat} is not the dominant bonding term, it is certainly far from being negligible as it contributes ca. 30% to the total attraction between the deformed reactants.

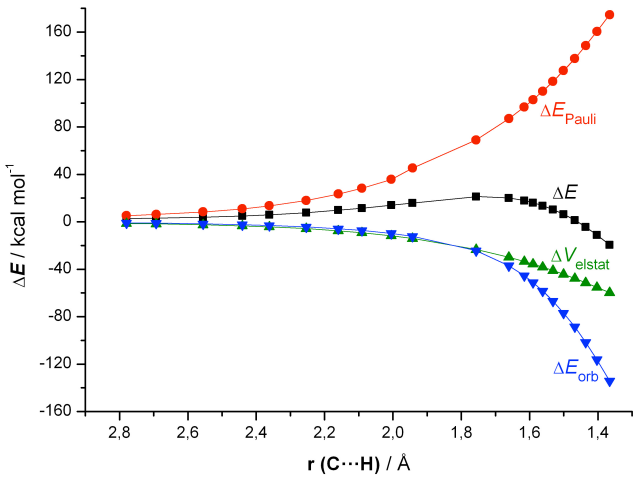

Fig 9. Energy Decomposition Analysis for the DGT reaction between ethane and ethene along the reaction coordinate projected onto the forming C···H bond. All data have been computed at the OLYP/TZ2P level. See reference 40.

The data in Figure 9 suggest that it would be possible to design low barrier DGT reactions if we could enhance the interaction energy between the reactants and/or reduce the destabilizing contribution of the strain term. Indeed, DGT processes where these requirements are satisfied have been described. For instance, in intramolecular type-II dyotropic reactions (see below) involving sesquinorbornanes,[43] the initial geometry of the reactant resembles that of the corresponding transition state, which significantly reduces the strain energy and leads to low barrier processes (ca. 20 kcal/mol).[44] Differently, in the MPV reduction of carbonyl groups, there occurs the formation of an intramolecular hydrogen-bond which approximates both reactants making the interaction energy between them stronger; as a consequence, the computed barrier for this process drops to ca. 25 kcal/mol.[40]

Similar and even lower activation barriers (9-24 kcal/mol) have been computed for the ruthenium catalysed Noyori-type hydrogenations of polar double bonds (i.e. ketones, aldehydes and imines) which also involve a double hydrogen atom migration.[45] There is general agreement that (i) a metal hydride (M–H) intermediate is the reactive species in the transformation and (ii) the hydride delivery to the electrophilic carbon atom takes place via a six-membered pericyclic transition structure[46] (similar to $\mathbf{TS_{Ru}}$, Figure 10) which resembles that for the DGT between ethene and ethane (see above). Indeed, this type of transition states also exhibit in-plane aromaticity (computed NICS values ranging from –8.0 to –16.0 ppm, depending on the substrate).[45] Similarly to the MPV reduction of carbonyl groups (see above), the presence of a heteroatom in the acceptor moiety is responsible for a remarkable increase of the interaction energy between the reactants which can compensate the destabilizing effect of the strain energy associated with the deformation of the initial reagents. As a consequence, low reaction barriers were computed for these transition metal mediated DGT reactions.[45]

The above examples nicely illustrate the utility of the combined ASM/EDA method to understand the physical factors controlling the barrier heights of different fundamental processes (like DGT reactions). But, maybe more important, they also show that these factors can be modified in order to design more favourable transformations (even prior to conducting the experiment).

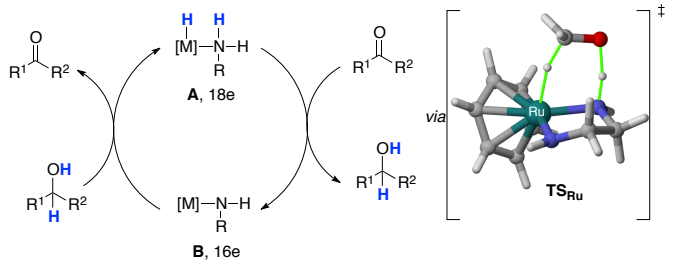

Fig 10. Noyori-type hydrogentation reaction of carbonyl groups.

Type-I Dyotropic Reactions

As a final example, we have selected a particular type of DGT reactions known as dyotropic rearrangements. These processes are defined as non-catalysed pericyclic valence isomerizations which involve the intramolecular and simultaneous migration of two σ-bonds. According to the original classification by M. T. Reetz,[47] in type-I dyotropic rearrangements, the migrating atoms or groups interchange their relative molecular positions, whereas in type-II dyotropic processes, they both move to new bonding sites.[48] Since this definition in the 70's, a good number of new processes, even involving transition metals and excited states, have been reported thus widening the mechanistic scope to new reaction pathways well away from the original definition of uncatalysed and concerted transformations.[48]

One of the most representative type-I dyotropic reactions involves the 1,2-shift of vicinal dibromides, initially described in steroideal compounds,[49] which proceeds with inversion of configuration at both carbon atoms (Figure 11a). This interesting reaction is reported to proceed concertedly through a four-membered ring transition state involving the simultaneous migration of both bromine atoms (Figure 11b).[50] Despite that, very little is known about the factors controlling the barrier heights of this process and the migratory aptitude of different X groups (Figure 11b). Hence, we decided again to apply the combined ASM/EDA method to gain more insight into the intimacies of this synthetically useful process.[51]

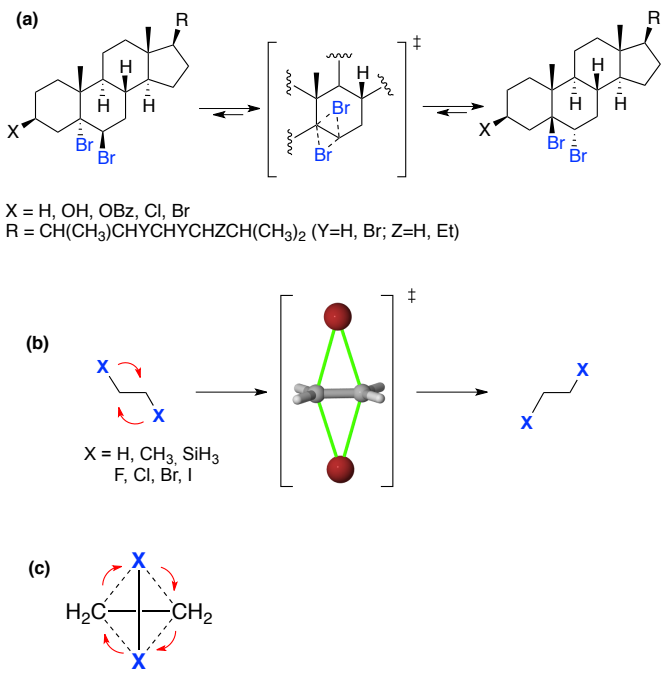

Fig 11. (a) Type-I dyotropic reaction in cholestanes. (b) Dyotropic rearrangement involving vicinal 1,2-shifts in substituted ethanes. (c) Rotation of the [X···X] fragment relative to the $H_2C{=}CH_2$ fragment used in the ASM.

However, the ASM method was originally conceived for understanding bimolecular processes which correspond to a two-fragment picture.[11,12] Therefore, we had to expand the scope of the method to study these intramolecular (i.e. uni-molecular) type-I dyotropic rearrangements. To this end, the considered type-I 1,2-dyotropic reactions can be conceived as the interconversion between two very strongly bound reactant complexes of X_2 + $H_2C{=}CH_2$. In fact, the progress of the reaction indeed strongly resembles a rotation of the [X···X] fragment (or "reactant") relative to the $H_2C{=}CH_2$ fragment (or "reactant"), as schematically shown in Figure 11c. This approach turns out to provide detailed insight into trends in activation energies by separating them into trends in X_2 and $H_2C{=}CH_2$ rigidity and C–X bonding. Hence, in this picture the barrier of the 1,2-dyotropic reaction arises from the *change* in strain of and in interaction between X_2 and $H_2C{=}CH_2$ as one goes from X–CH_2–CH_2–X to the corresponding transition state. Therefore, in this particular case: $\Delta E^{\ddagger} = \Delta\Delta E_{strain}^{\ddagger} + \Delta\Delta E_{int}^{\ddagger}$.

Our calculations indicate that the migratory aptitude of the X groups/atoms in this dyotropic movement increases in the order: H < CH_3 < SiH_3 << F < Cl< Br < I.[51] Therefore, the process can be considered as not feasible when a hydrogen atom, a methyl or a SiH_3 group is involved in the dyotropic movement (activation barrier > 100 kcal/mol). In contrast, the computed activation barriers are much lower when X = halogen atom, observing the lowest activation barriers for X = Br and I (32 and 25 kcal/mol, respectively). This is mainly ascribed to an additional stabilizing donor-acceptor orbital interaction between the halogen lone pairs and the π* orbital of ethylene fragment, which completes the pericyclic circuit but which is absent for H, CH_3, and SiH_3.[51]

Interestingly, the ASM analyses show that the change in the strain energies, $\Delta\Delta E_{strain}$, when going from the initial reactant to the transition state is stabilizing. This is mainly due to the fact that in the respective saddle points, the C_2H_4 fragment adopts an almost planar geometry which closely resembles its intrinsically preferred ethylene structure. Differently, the change in the interaction energies, $\Delta\Delta E_{int}$, is clearly destabilizing, which can be ascribed to the partial dissociation of the C–X bond in the transition state. Indeed, the EDA method reveals that the orbital and electrostatic interaction terms become less stabilizing and Pauli repulsion less destabilizing if one goes from the reactant to the transition state (Figure 12). The above trends are all due to the elongation of the original C–X bonds along the reaction coordinate. Therefore, it can be concluded that the weakening in the interaction energy ΔE_{int}, that derives from partial C–X bond breaking in the transition state, constitutes the major factor controlling the barrier of the 1,2-dyotropic migration. This finding becomes evident from the very good linear relationship found when plotting the computed activation barriers $\Delta E^{\ddagger}$ *versus* the change in the transition state interaction energy $\Delta\Delta E_{int}^{\ddagger}$. This result indicates that the trends in reactivity on variation of X in these particular 1,2-shifts can be rationalized in terms of how sensitive the C–X interaction is towards adopting the transition state geometry. In other words: the softer the C–X bond, the lower the barrier.

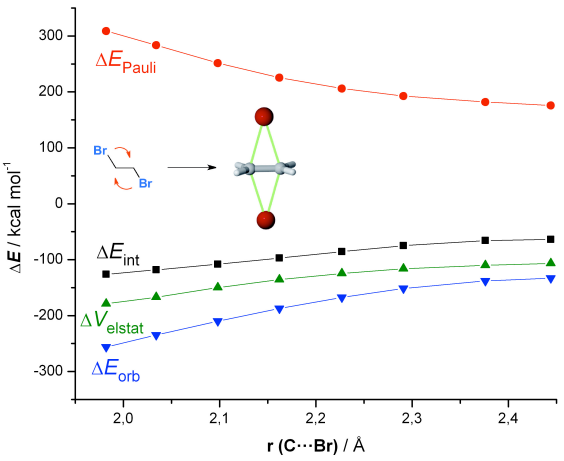

Fig X. Energy Decomposition Analysis for the type-I dyotropic rearrangement involving 1,2-dibromoethane along the reaction coordinate projected onto the C···Br bond. All data have been computed at the OLYP/TZ2P level. See reference 51.

The latter results clearly show that the ASM/EDA method can be efficiently applied not only to bimolecular processes but also to unimolecular transformations. Therefore, the factors governing any conceivable reaction can be studied within this methodology.

Conclusions and Outlook

In this Perspective article, we provide an overview of the application of the combined ASM/EDA methods to selected pericyclic reactions, in particular, Diels-Alder and double group transfer reactions. This methodology, which is based on accurate quantum chemical calculations, allows for a deeper, quantitative understanding of the physical factors that control the barrier heights and reactivity trends of any chemical transformation. Indeed, this method constitutes a new way of studying fundamental processes in organic and organometallic chemistry which complements the more traditional, widely used methods, such as the highly popular FMO theory.

It becomes clear that the insight provided by the ASM/EDA method can be used *a posteriori* to interpret the outcome of a chemical transformation. But, maybe more importantly, given the tremendous predictive ability of the methodology, it may serve to rationally design more efficient processes prior the experiment.

In our opinion, our current view of many fundamental processes in Chemistry will be complemented and even modified by the insights emerging from the ASM/EDA method.

Acknowledgements

Financial support from the Spanish MINECO (CTQ2010-20714-C02-01/BQU and Consolider-Ingenio 2010, CSD2007-00006) and CAM (S2009/PPQ-1634) is gratefully acknowledged. We thank Prof. F. M. Bickelhaupt for his continuous support and helpful comments.

Notes and references

[a] Departamento de Química Orgánica, Facultad de Ciencias Químicas, Universidad Complutense de Madrid, 28040-Madrid, Spain. Fax: +34-913944310. E-mail: israel@quim.ucm.es

1 S. Sankararaman, *Pericyclic Reactions–A Textbook: Reactions, Applications and Theory*; Wiley: Weinheim, 2005.
2 See also Rzepa's blog on pericylic reactions: http://www.ch.ic.ac.uk/local/organic/pericyclic/index.html
3 For a review, see: (a) D. H. Ess, G. O. Jones and K. N. Houk, *Adv. Synth. Catal*. 2006, **348**, 2337. See also, (b) K. N. Houk, *Acc. Chem. Res*. 1975, **8**, 361.
4 (a) K. Fukui and H. Fujimoto, *Bull. Chem. Soc. Jpn*., 1967, **40**, 2018. (b) K. Fukui and H. Fujimoto, *Bull. Chem. Soc. Jpn*., 1969, **42**, 3399. (c) K. Fukui, *Fortschr. Chem. Forsch*., 1970, **15**, 1. (d) K. Fukui, *Acc. Chem. Res*., 1971, **4**, 57. (e) K. Fukui, *Angew. Chem. Int. Ed. Engl*., **1982**, *21*, 801.
5 R. B. Woodward and R. Hoffmann, *The Conservation of Orbital Symmetry*, Verlag, Chemie, GmbH: Weinheim, 1970.
6 I. Fleming, *Frontier Orbitals and Organic Chemical Reactions*; Wiley: New York, 1976.
7 See, for instance: (a) S. D. Kahn, C. F. Pau, L. E. Overman and W. J. Hehre, *J. Am. Chem. Soc*., 1986, **108**, 7381. (b) C. Spino, H. Rezaei and Y. L. Dory, *J. Org. Chem*., 2004, **69**, 757. (c) B. R. Ussing, C. Hang and D. A. Singleton, *J. Am. Chem. Soc*., 2006, **128**, 7594.
8 (a) P. Geerlings, F. De Proft and W. Langenaeker, *Chem. Rev*., 2003, **103**, 1793. (b) P. Geerlings, P. W. Ayers, A. Toro-Labbé, P. K. Chattaraj and F. de Proft, *Acc. Chem. Res*., 2012, **45**, 683.

9 (a) A. Pross and S. Shaik, *Acc. Chem. Res*., 1983, **16**, 363. (b) R. Hoffmann, S. Shaik and P. C. Hiberty, *Acc. Chem. Res*., 2003, 36, 750. (c) S. Shaik and P. C. Hiberty, *A Chemist's Guide to Valence Bond Theory,* Wiley-Interscience, Hoboken, New Jersey, 2007.

10 R. A. Marcus, *Annu. Rev. Phys. Chem*., 1964, **15**, 155.

11 (a) F. M. Bickelhaupt, *J. Comput. Chem*., 1999, **20**, 114. (b) A. Diefenbach and F. M. Bickelhaupt, *J. Chem. Phys*., 2001, **115**, 4030. (c) A. Diefenbach and F. M. Bickelhaupt, *J. Phys. Chem. A,* 2004, **108**, 8460. (d) A. Diefenbach, G. T. de Jong and F. M. Bickelhaupt, *J. Chem. Theory Comput*., 2005, **1**, 286. (e) J. N. P. van Stralen and F. M. Bickelhaupt, *Organometallics,* 2006, **25**, 4260. (f) G. T. de Jong and F. M. Bickelhaupt, Chemphyschem, 2007, **8**, 1170. (g) G. T. de Jong and F. M. Bickelhaupt, *J. Chem. Theory Comput*., 2007, **3**, 514. (h) A. P. Bento and F. M. Bickelhaupt, *J. Org. Chem*., 2008, **73**, 7290. (i) I. Fernández, G. Frenking and E. Uggerud, *Chem. Eur. J*., 2009, **15**, 2166. (j) W.-J. van Zeist and F. M. Bickelhaupt, *Org. Biomol. Chem*., 2010, **8**, 3118. (k) I. Fernández, G. Frenking and E. Uggerud, *J. Org. Chem*., 2010, **75**, 2971. (l) I. Fernández, F. M. Bickelhaupt and E. Uggerud, *J. Org. Chem*., 2013, **78**, 8574.

12 Selected representative examples: (a) D. H. Ess and K. N. Houk, *J. Am. Chem. Soc*., 2007, **129**, 10646. (b) D. H. Ess, and K. N. Houk, *J. Am. Chem. Soc*., 2008, **130**, 10187. (c) R. S. Paton, S. Kim, A. G. Ross, S. J. Danishefsky and K. N. Houk, *Angew. Chem. Int. Ed*., 2011, **50**, 10366. (d) F. Liu, R. S. Paton, S. Kim, Y. Liang, and K. N. Houk, *J. Am. Chem. Soc*., 2013, **135**, 15642.

13 (a) K. Fukui, *Acc. Chem. Res*., 1981, **14**, 363. (b) C. González and H. B. Schlegel, *J. Phys. Chem*., 1990, **94**, 5523.

14 (a) F. M. Bickelhaupt and E. J. Baerends, *Rev. Comput. Chem*., 2000, **15**, 1. (b) M. Lein and G. Frenking, *Theory and Applications of Computational Chemistry* (Eds.: E. D. Clifford, G. Frenking, S. K. Kwang, E. S. Gustavo), Elsevier, Amsterdam, 2005, pp. 291. (c) M. von Hopffgarten and G. Frenking, *WIREs Comput. Mol. Sci*., 2012, **2**, 43.

15 T. Ziegler, A. Rauk, *Theor. Chim. Acta,* **1977**, *46*, 1.

16 K. Morokuma, *J. Chem. Phys*., **1971**, *55*, 1236.

17 Representative examples: (a) C. Esterhuysen, G. Frenking, *Theor. Chem. Acc*., 2004, **111**, 381. (b) A. Kovács, C. Esterhuysen, G. Frenking, *Chem. Eur. J*., 2005, **11**, 1813. (c) A. Krapp, F. M. Bickelhaupt, G. Frenking, *Chem. Eur. J*., 2006, **12**, 9196. (d) I. Fernández, G. Frenking, *Chem. Eur. J*., 2006, **12**, 3617. (e) a) I. Fernández, G. Frenking, *Faraday Discuss*., 2007, **135**, 403. (f) S. C. A. H. Pierrefixe, F. M. Bickelhaupt, *Chem. Eur. J.,* 2007, **13**, 6321. (g) I. Fernández, M. Duvall, J. I-C. Wu, P. v. R. Schleyer, G. Frenking, *Chem. Eur. J*., **2011**, *17*, 2215. (h) I. Fernández and G. Frenking, *Phys. Chem. Chem. Phys*., 2012, **14**, 14869. (i) I. Fernández, J. I. Wu, P. v. R. Schleyer, *Org. Lett*., 2013, **15**, 2990.

18 Some examples: G. Frenking, K. Wichmann, N. Fröhlich, C. Loschen, M. Lein, J. Frunzke, V. M. Rayón, *Coord. Chem. Rev*., 2003, **238–239**, 55. (b) B. Buchin, C. Gemel, T. Cadenbach, I. Fernández, G. Frenking and R. A. Fischer, *Angew. Chem. Int. Ed*., 2006, **45**, 5207. (c) I. Fernández and G. Frenking, *Chem. Eur. J*., 2007, **13**, 5873. (d) T. Cadenbach, T. Bollermann, C. Gemel, I. Fernández, M. von Hopffgarten, G. Frenking, and R. A. Fischer, *Angew. Chem. Int. Ed*., 2008, **47**, 9150. (e) T. Cadenbach, T. Bollermann, C. Gemel, M. Tombul, I. Fernández, M. von Hopffgarten, G. Frenking, and R. A. Fischer, *J. Am. Chem. Soc*., 2009, **131**, 16063. (f) M. Parafiniuk and M. P. Mitoraj, *Organometallics*, 2013, **32**, 4103.

19 See, for example: (a) C. Fonseca Guerra, F. M. Bickelhaupt, J. G. Snijders and E. J. Baerends, *Chem. Eur. J.,* 1999, **5**, 3581-3594. (b) C. Fonseca Guerra, T. van der Wijst and F. M. Bickelhaupt, *Chem. Eur. J.,* 2006, **12**, 3032-3042. (c) C. Fonseca Guerra, Z. Szekeres, F. M. Bickelhaupt, *Chem. Eur. J.,* 2011, **17**, 8816. (d) C. Fonseca Guerra, H. Zijlstra, G. Paragi, F. M. Bickelhaupt, *Chem. Eur. J.,* 2011, **17**, 12612.

20 (a) S. Kobayashi, K. A. Jorgensen, Eds. *Cycloaddition Reactions in Organics Synthesis*; Wiley-VCH: Weinheim, 2001. (b) For a review on the applications of Diels-Alder reactions in synthesis, see: K. C. Nicolaou, S. A. Snyder, T. Montagnon, G. Vassilikogiannakis *Angew. Chem. Int. Ed.,* 2002, **41**, 1668.

21 K. Alder, G. Stein, *Justus Liebigs Ann. Chem*. 1934, **514**, 1.

22 (a) A. Wassermann, *J. Chem. Soc*., 1935, **825**, 1511. (b) A. Wassermann, *Trans. Faraday Soc*., 1939, **35**, 841.

23 R. B. Woodward and H. Baer, *J. Am. Chem. Soc*. 1944, **66**, 645.

24 (a) A. L. Ringer, M. S. Figgs, M. O. Sinnokrot and C. D. Sherrill, *J. Phys. Chem. A*, 2006, **110**, 10822. (b) S. Maity, R. Sedlak, P. Hobza and G. N. Patwari, *Phys. Chem. Chem. Phys*., 2009, **11**, 9738.

25 C. S. Wannere, A. Paul, R. Herges, K. N. Houk, H. F. Schaefer, III and P. v. R. Schleyer, *J. Comput. Chem*., 2007, **28**, 344.

26 R. Hoffmann and R. B. Woodward, *J. Am. Chem. Soc*., 1965, **87**, 4388.

27 A. Arrieta, F. P. Cossío and B. Lecea, *J. Org. Chem*., 2001, **66**, 6178.

28 I. Fernández and F. M. Bickelhaupt. *J. Comput. Chem*., 2013, DOI: 10.1002/jcc.23500.

29 L. M. Stephenson, D. E. Smith and S. P. Current, *J. Org. Chem*., 1982, **47**, 4170.

30 I. Fernández, M. Solà and F. M. Bickelhaupt, *Chem. Eur. J.*, 2013, **19**, 7416.

31 (a) *Fullerenes: From Synthesis to Optoelectronic Properties* (Eds.: D. M. Guldi, N. Martín), Kluver, Dordrecht, 2002. (b) *Fullerenes. Principles and Applications* (Eds.: F. Langa, J.-F. Nierengarten), RSC, Cambridge, 2011. (c) N. Martín, *Chem. Commun*., 2006, 2093.

32 (a) R. Taylor, *The Fullerenes* (Eds.: H. W. Kroto, D. R. M. Walton), Cambridge University Press, Cambridge, 1993, pp. 87–101. (b) A. Hirsch, *The Chemistry of the Fullerenes*, Thieme, Stuttgart, **1994**.

33 (a) L. M. Giovane, J. W. Barco, T. Yadav, A. L. Lafleur, J. A. Marr, J. B. Howard and V. M. Rotello, *J. Phys. Chem*., 1993, **97**, 8560. (b) L. S. K. Pang and M. A. Wilson, *J. Phys. Chem*., 1993, **97**, 6761.

34 (a) J. Mestres, M. Duran and M. Solá, *J. Phys. Chem*. 1996, **100**, 7449. (b) A. Chikama, H. Fueno and H. Fujimoto, *J. Phys. Chem*., 1995, **99**, 8541. (c) X.-F.Gao, C.-X. Cui and Y.-J. Lui, *J. Phys. Org. Chem*., 2012, **25**, 850.

35 (a) S. Hülnig, H. R. Müller and W. Thier, *Angew. Chem. Int. Ed. Engl.,* 1965, **4**, 271. (b) E. W. Garbisch, Jr., S. M. Schildcrout, D. B. Patterson, C. M. Sprecher, *J. Am. Chem. Soc*., 1965, **87**, 2932. (c) M. Franck-Neumann and C. Dietrich-Buchecker, *Tetrahedron Lett*., 1980, 671.

36 (a) H. Meerwein and R. Schmidt, *Justus Liebigs Ann. Chem*., 1925, **444**, 221. (b) W. Ponndorf, *Angew. Chem*., 1926, **39**, 138. This latter process has been proposed to evolve through a cyclic six-membered transition state at elevated temperatures. See, (c) L. Sominsky, E.

Rozental, H. Gottlieb, A. Gedanken and S. Hoz, *J. Org. Chem*., 2004, **69**, 1492.

37 I. Fernández, M. A. Sierra and F. P. Cossío, *J. Org. Chem.*, 2007, **72**, 1488.

38 (a) I. Morao, B. Lecea and F. P. Cossío, *J. Org. Chem*., 1997, 62, 7033. (b) F. P. Cossío, I. Morao, H. Jiao and P. von R. Schleyer, *J. Am. Chem. Soc*., 1999, **121**, 6737. (c) I. Fernández, M. A. Sierra and F. P. Cossío, *J. Org. Chem*., 2006, **71**, 6178.

39 Z. Chen, C. S. Wannere, C. Corminboeuf, R. Puchta, P. v. R. Schleyer, *Chem. Rev*., 2005, **105**, 3842.

40 (a) I. Fernández, F. M. Bickelhaupt and F. P. Cossío, *Chem. Eur. J*., 2009, **15**, 13022. (b) I. Fernández and F. P. Cossío, *Curr. Org. Chem*., 2010, **14**, 1578.

41 I. Fernández, F. P. Cossío and F. M. Bickelhaupt, *J. Org. Chem*., 2011, **76**, 2310.

42 I. Fernández and F. M. Bickelhaupt, *J. Comput. Chem.*. 2012, **33**, 509.

43 (a) K. Mackenzie, J. A. K. Howard, S. Mason, E. C. Gravett, K. B. Astin, S. X. Liu, A. S. Batsanov, D. Vlaovic and J. P. Maher, *J. Chem. Soc., Perkin Trans. 2*, 1993, **6**, 1211. (b) K. N. Houk, J. Y. Li, M. A. McAllister, G. A. O'Doherty, L. A. Paquette, W. Siebrand and Z. K. Smedarchinal, *J. Am. Chem. Soc*., 1994, **116**, 10895.

44 G. Frenking, F. P. Cossío, M. A. Sierra and I. Fernández, *Eur. J. Org. Chem*., 2007, 5410.

45 O. Nieto Faza, C. Silva López and I. Fernández, *J. Org. Chem*., 2013, **78**, 5669.

46 (a) C. A. Sandoval, T. Ohkuma, K. Muñiz and R. Noyori, *J. Am. Chem. Soc*., 2003, **125**, 13490. (b) O. Nieto Faza, I. Fernández and C. Silva López, *Chem. Comm*. 2013, **49**, 4277, and references therein.

47 (a) M. T. Reetz, *Angew. Chem. Int. Ed. Engl.,* 1972, **11**, 130. (b) M. T. Reetz, *Tetrahedron,* 1973, **29**, 2189.

48 For a recent review on dyotropic reactions, see: I. Fernández, F. P. Cossío and M. A. Sierra, *Chem. Rev*., 2009, **109**, 6687, and references therein.

49 C. A. Grob and S. Winstein, *Helv. Chim. Acta* 1952, **35**, 782.

50 (a) A. Frontera, G. Suñer and P. M. Deyá, *J. Org. Chem*., 1992, **57**, 6731. (b) J.-W. Zou and C.-H. Yu, *J. Phys. Chem. A,* 2004, **108**, 5649. (c) I. Fernández, M. A. Sierra and F. P. Cossío, *Chem. Eur. J*., 2006, **12**, 6323.

51 I. Fernández, F. M. Bickelhaupt and F. P. Cossío, *Chem. Eur. J.,* 2012, **18**, 12395.

Biographical Sketch

Israel Fernández (Madrid, 1977) studied Chemistry at the Universidad Complutense of Madrid (UCM). In 2005, he earned his Ph.D. (with honors) at the UCM under the supervision of Prof. Miguel A. Sierra receiving the Lilly-Young Researcher Award. After that, he joined the Theoretical and Computational Chemistry group of Prof. Gernot Frenking at the Philipps Universität Marburg as a postdoctoral researcher. In 2009, he received the Young-Researcher Award from the Spanish Royal Society of Chemistry and the Julián Sanz del Río award in 2011. At present, I.F. is *Profesor Contratado Doctor* at the UCM. His current research includes the experimental and computational study of the bonding situations and reaction mechanisms of organic and organometallic compounds with special interest in C-C bond forming processes